- Technical Paper -

EFFECT OF STIRRUPS ARRANGEMENT ON FAILURE OF BEAM COLUMN JOINT WITH MECHANICAL ANCHORAGES BY 3D DISCRETE MODEL

Liyanto EDDY[*1] and Kohei NAGAI[2]

ABSTRACT

The use of mechanical anchorage is still limited because the performance has not been well understood. In this study, a 3D meso-scale discrete analysis is conducted in order to investigate the effect of the stirrups arrangement on the failure of beam column joints with mechanical anchorages through the comparison with the experimental results. The simulation results are in good agreement with the experimental results. Based on the simulation results, the causes of major cracks are described. Eventually, the failure process of beam column joints with mechanical anchorages has been revealed through the study of the internal stress and the cracking pattern of RBSM.

Keywords: knee-joints, RBSM, mechanical anchorage, anchorage failure, local re-bar arrangement

1. INTRODUCTION

Reinforcement congestion, particularly occurs in a beam column joint, can cause difficulties during compaction, resulting a poor quality of concrete. One way to reduce the reinforcement congestion in a beam column joint is by using mechanical anchorage because the length of the anchorage can be reduced and the detail of the anchorage is simpler than that of conventional hooked bars (Fig.1). However, the use of mechanical anchorage is still limited in the reinforced concrete members with thin concrete cover because the performance has not been well understood [1].

Based on the previous experimental work, conducted by Yoshimura *et al.* [2], different failure pattern was observed due to different local reinforcement arrangement, for example: brittle behavior, local splitting failure, was observed both in case of no stirrup provided along the anchorage and in case of stirrups provided only at the end of the anchorage and ductile behavior, flexural failure, was observed in case of stirrups provided at the end and along the anchorage. Hence, the local reinforcement arrangement and the local failure significantly affect the macroscopic behavior and the behavior was not so easy to be understood through experimental works. Simulation can be a beneficial tool to understand the behavior.

In this study, a meso-scale analysis of reinforced concrete members by a 3D discrete element analysis, called RBSM, is conducted. The study by a 3D meso-scale discrete analysis is useful since the reinforcement arrangement can be modeled in an accurate manner, local failure can be predicted precisely as the result of the discontinuous deformation of concrete at meso-scale level, and cracks can be introduced as the displacement between two elements. Moreover, Wang *et al.* [3] successfully simulated different crack patterns with different anchorage systems of knee-joints by RBSM. Eventually, the purpose of this study is to investigate the effect of the local reinforcing bars arrangement, especially the arrangement of stirrups, along the anchorages on the failure mechanism of the beam column joint by 3D discrete model, through the comparison with experimental results. Capacity, cracking pattern, and local internal stress condition of simulation results will be investigated.

Fig.1 Mechanical anchorage

2. ANALYSIS METHOD

In this study, the simulation is carried out by a three dimensional RBSM, proposed by Kawai *et al.* [4]. In RBSM, a three dimensional reinforced concrete model is meshed into rigid bodies. Each rigid body consists of six degree of freedoms, i.e. three translational degrees of freedom and three rotational degrees of freedom at some points within its interior and connects with other rigid bodies by three springs, i.e. two shear springs and one normal spring. As the propagation of cracks in reinforced concrete is one of the most important factors in investigating the behavior of reinforced concrete members, the mesh arrangement of the model in RBSM is important. In order to prevent cracks propagated in a non-arbitrary direction, a random geometry, called Voronoi Diagram, is used for the element meshing. The concrete element size is modeled

*1 Graduate Student, Department of Civil Engineering, The University of Tokyo, Tokyo, Japan, JCI Student Member. Email: eddy@iis.u-tokyo.ac.jp

*2 Associate Professor, International Center for Urban Safety Engineering, Institute of Industrial Science, The University of Tokyo, Tokyo, Japan, JCI Member

Table.1 Detail of numerical models

Case	Parameter	Material Properties of Concrete			Number of Elements	Maximum Load	
		Compression $f`_c$ (MPa)	Tension f_t (MPa)	Elasticity E_s (MPa)		EXP (kN)	ANA (kN)
AL2	No stirrups	30.8	2.43	27900	756638	94.5	91.1
BL1	Stirrups at the end of anchorage	33.2	2.58	24200	766375	120.1	103.5
BL2	Stirrups at the end of anchorage and along anchorage	33.5	3.09	25800	805706	134.2	117.1

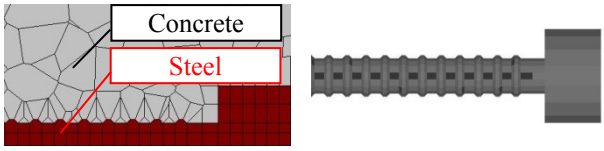

(a) Cross section (b) Model of 3D Rebar

Fig.2 Mesh arrangement of concrete and re-bar

approximately 10^3 to 20^3 mm^3 that is similar to the aggregate size. The geometry of steel elements is modeled in an accurate manner, by modeling a 3D arrangement of reinforcing bar, to properly account for the interlock between the reinforcing bar and concrete. Mesh arrangement of concrete and steel at meso-scale in this study is shown in Fig.2. To model a 3D reinforced concrete member, two types of elements are used, i.e. concrete element and steel element. The properties of the springs are determined so that the elements, when combined together, enable to predict the behaviour of the model as accurate as that of the experimental result. In this study, the simulation system, developed by Nagai *et al.* [5], is used. Fig.3 shows the constitutive model of the concrete element. At steel-concrete interface, the constitutive models of the normal spring and shear spring are considered to be the same as those of the concrete element. To consider the interface as a weak region, the tensile strength of the interface element is assumed to be half of that of concrete element.

In addition, the applicability of the analysis method to simulate the confinement effect by stirrups has been confirmed by Hayashi *et al.* [6].

3. DETAIL OF NUMERICAL SIMULATIONS

3.1 Numerical Model

Simulations were conducted for experiments, carried out by Yoshimura *et al.* [2]. The purpose of the experiments was to clarify the performance of the mechanical anchorage, embedded in a beam column joint, with different types of local reinforcing bars arrangement. In this study, the effect of the stirrups arrangement along the anchorage is the main focus.

Numerical models are listed in Table.1. Three numerical models, with different stirrups arrangements, were modeled. For the recognition of the variables in each model, the same notations with the experimental specimens are used. AL2 signifies that no stirrup was provided along the anchorages, BL1 signifies that stirrups were provided only at the end of the anchorage, and BL2 signifies that stirrups were provided at the end of the anchorage and along the anchorage.

3.2 Geometry of Numerical Model

Fig.4 shows the geometry of the numerical models. The same dimensions, as the experimental specimens, were modeled. As the comparison, the detail of the experimental specimens, conducted by Yoshimura *et al.* [2] is shown in Fig.5.

The reinforcement arrangement of numerical models was modeled as the same as that of experimental specimens. Deformed bars of 19 mm and 22 mm were used as the main reinforcements of column and beam, respectively. However, for the simplification of the model and in order to reduce the computational time, plain bar was used for modeling all stirrups. Plain bars of 10 mm were used as the stirrups of both column and beam. Plain bars of 13 mm were used as the stirrups at the end of the anchorages and along the anchorages in the beam column joint. In this simulation, the function of stirrups in the beam column joint is to provide the

Table.2 Material properties of reinforcing bars

Re-bars	Function	Numerical Model	Yield Strength MPa	Modulus of Elasticity MPa
D22	Main reinforcements of column	AL2	377	183000
		BL1-BL2	392	193000
D19	Main reinforcements of beam	AL2	435	184000
		BL1-BL2	458	199000
D13	Stirrups at the end of anchorage	BL1-BL2	806	193000
D13	Stirrups along the anchorage	BL2	368	197000
D10	Stirrups of beam and column	AL2	363	203000
		BL1-BL2	368	197000

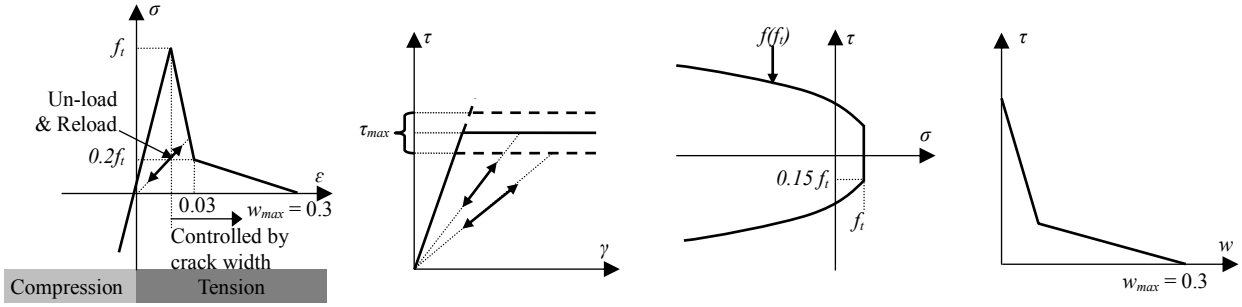

(a) Normal spring (b) Shear spring (c) Failure criterion (d) Shear reduction

Fig.3 Constitutive model of concrete

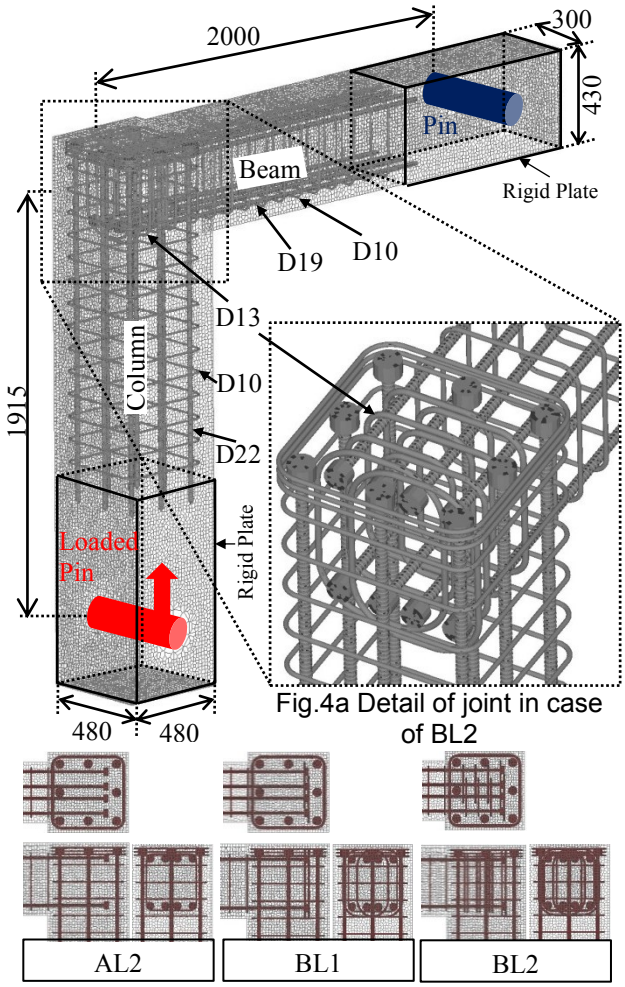

Fig.4a Detail of joint in case of BL2

Fig.4 Geometry and boundary condition of numerical models (Units: mm)

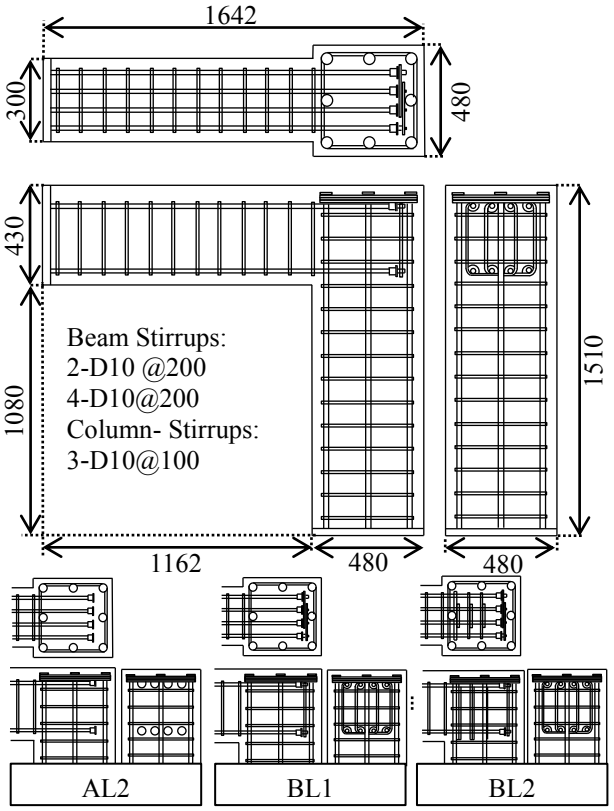

Fig.5 Experimental specimens

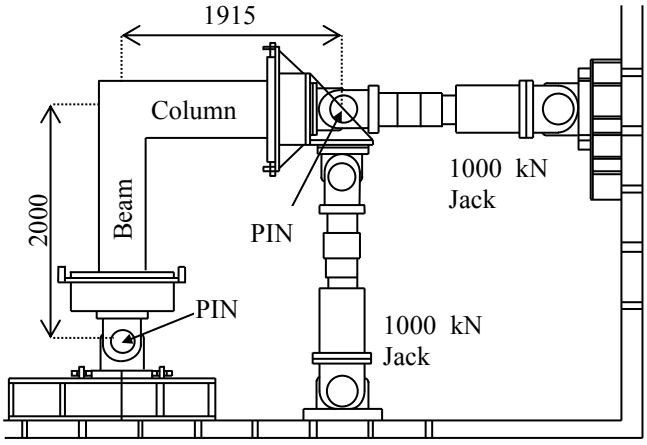

Fig.6 Experimental setup (Units: mm)

confinement effect, so that the propagation of main cracks in the beam column joint will not be affected significantly.

Material properties of re-bars of each model are shown in Table.2. The material properties of numerical models are the same as those of experimental specimens.

3.3 Boundary Condition

Boundary conditions of numerical models are shown in Fig.4. As the comparison, the detail of the experimental setup is shown in Fig.6. Steel plates were modeled located at the end of the beam and the column. The stiffness of the steel plates was assumed rigid enough, so that the deformation of the steel plates will be prevented. In order to model the hinged condition, a pin element is introduced, located in the steel plates. Furthermore, in a pin element, forces are transferred only through normal springs of the pin element.

Cyclic load was applied to the experimental specimens. However, since brittle failure was observed only when the beam column joint is loaded by a moment that tends to close the beam column joint and the stirrups arrangement may affect significantly on the anchorage performance under this load, only push load case will be discussed in this study. Monotonically displacement-load controlled was applied to the pin, located at the end of the column and fix condition was assumed at the pin, located at the end of the beam.

4. RESULTS AND DISCUSSION

4.1 Load-Displacement Relationships

Load-displacement relationships of experimental specimens are compared with those of numerical models. Fig.7 and Fig.8 show the load-displacement relationships of experimental specimens and numerical models respectively. The load of load-displacement relationships, both experimental specimens and numerical models, was determined based on the load which was applied to the pin, located at the end of the column. Meanwhile, the displacement of load-displacement relationships, both experimental specimens and numerical models, was calculated based on the drift angle. Table.1 shows the maximum loads of experimental specimens and numerical models.

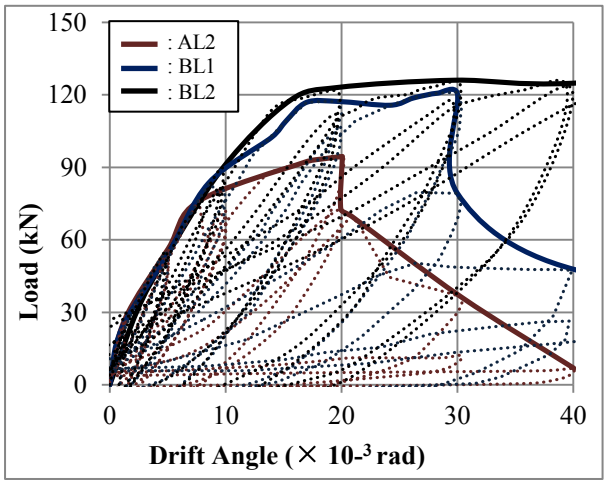

Fig.7 Load-displacement relationships of experimental specimens

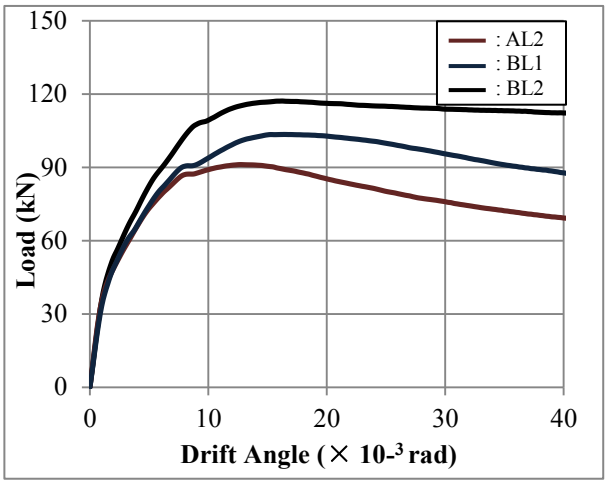

Fig.8 Load-displacement relationships of numerical models

The maximum loads of numerical models are roughly the same as those of experimental specimens, i.e. approximately 4-14% difference. In case of AL2, the simulation is underestimate by 4%, in case of BL1, the simulation is underestimate by 14%, and in case of BL2, simulation is underestimate by 13%. Thus, the maximum loads of numerical models coincide well with those of experimental specimens.

Based on the load-displacement relationship of simulation results, the maximum load of BL1 is higher than that of AL2. Simulation results predict that after exceeding the maximum load, the load decreases significantly in both cases. Experimental results also observed the same tendency. However, sudden drop in capacity after exceeding the maximum load could not be simulated well in the simulation.

In case of BL2, simulation result predicts that the maximum load of BL2 is higher than that of AL2 and BL1. After exceeding the maximum load, the load does not decrease significantly. Experimental result also observed the same tendency.

4.2 Surface Cracks after Failure

Surface cracks of experimental specimens are compared with those of numerical models. Fig. 9 shows surface cracks of both numerical models and experimental specimens after failure. Generally, the crack patterns of numerical models are roughly the same as those of experimental specimens.

In all cases, simulation results predict that diagonal cracks, propagating from the anchorage plates of top longitudinal bars of the beam to the corner of the beam column joint and from the anchorage plates of middle longitudinal bars of the column to the corner of the beam column joint, occur in the numerical models. As the comparison, the same cracks were observed in the experimental specimens (①).

In case of AL2 and BL1, simulation results predict that damage occurs at the top surface of numerical models which indicates the anchorage failure in the beam column joint (②). However, the spalling of concrete at the top surface of numerical models could not be simulated as well as experimental specimens so that simulation could not simulate well the sudden drop

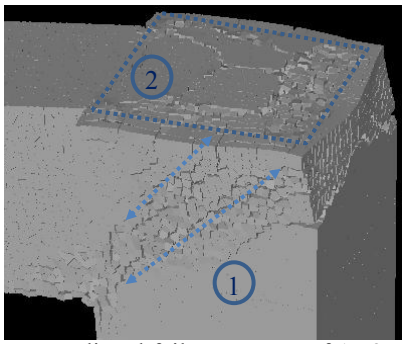

a. Predicted failure pattern of AL2 (Deformation×3)

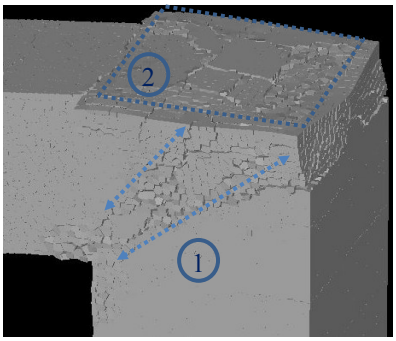

b. Predicted failure pattern of BL1 (Deformation×3)

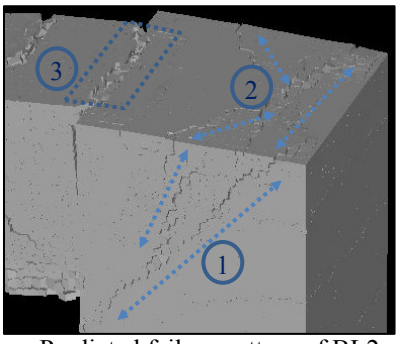

c. Predicted failure pattern of BL2 (Deformation×3)

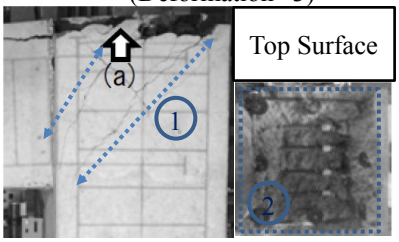

d. Observed failure pattern of AL2

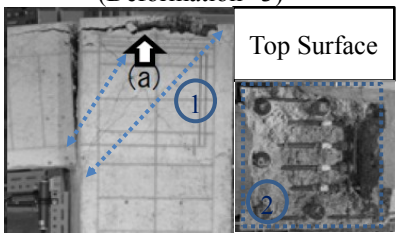

e. Observed failure pattern of BL1

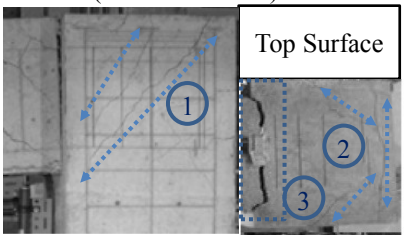

f. Observed failure pattern of BL2

Fig.9 Surface cracks after failure

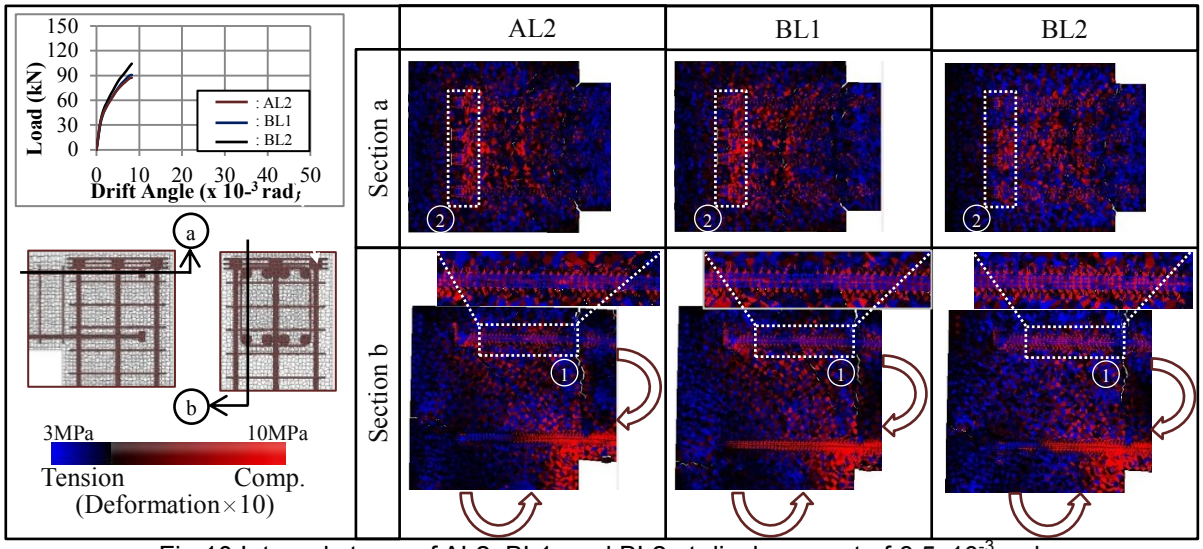

Fig.10 Internal stress of AL2, BL1, and BL2 at displacement of 8.5×10^{-3} rad

in capacity after exceeding the maximum load

In case of BL2, the simulation result predicts that cracks, along the end of the anchorage plates and propagating from the anchorage plates of top longitudinal bars of the beam to the side of the specimen, occur at the top surface of the numerical model (2). Meanwhile, the width of the flexural crack of BL2 is predicted larger than that of AL2 and BL1 that indicates the flexural failure in the beam column joint (3). The same cracks were also observed in the experimental specimens.

4.3 Internal Stress

Fig.10 and Fig.11 show the internal stress distribution of numerical models, at the displacement of 0.0085 rad and 0.025 rad, respectively. The deformation of the numerical models is enlarged by ten times. Blue color and red color indicate the tensile stress and the compressive stress of a normal spring, respectively.

When the load is relatively small, flexural cracks occur. As the load increases, at the displacement of 0.0085 rad, the compressive stress along the development length of BL2 is larger than that of BL1 and AL2 (1)and the compressive stress around the anchorage plates of BL2 is smaller than that of BL1 and AL2 (2). Meanwhile, there is no significant difference of the stress distribution along the anchorages between BL1 and AL2. These behaviors indicate that in case of BL2, the bond performance along the development length increases because of the effect of stirrups along the anchorages. Diagonal compressive stresses also develop from the anchorage plates, as the result of the bearing stress, to the compression zone of the beam. It is confirmed based on the simulation results that the capacity of BL2 increases because of the increase of the bond performance along the development length.

As the load increases, at the displacement of 0.025 rad, the diagonal compressive stresses have exceeded the capacity that causes diagonal cracks, propagating from the anchorage plates of top longitudinal bars of the beam to the corner of the beam column joint (3). The crack width of these cracks of BL2 is smaller than that of BL1 and AL2. The diagonal compressive stresses of BL2 is larger than that of AL2 and BL1 (4), caused by stirrups. Furthermore, in case of AL2 and BL1, because of no restriction along the anchorages, diagonal cracks open easier compared with that of BL2. As the result, diagonal compressive stresses are difficult to exist that causes the load decreases significantly after exceeding the maximum load. On the other hand, in case of BL2, because of the restriction along the anchorages, diagonal compressive stresses still

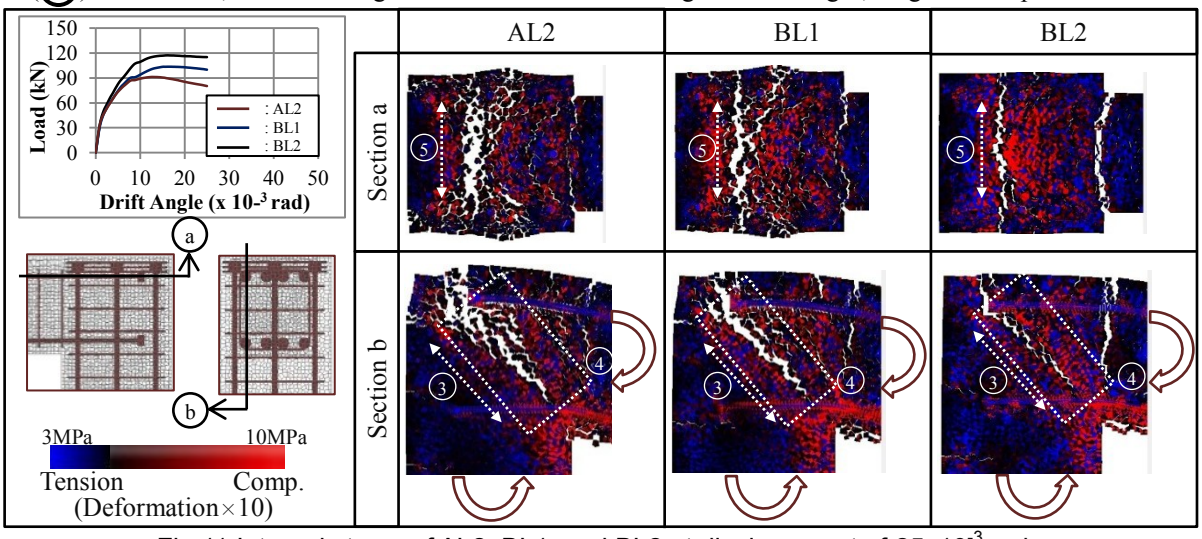

Fig.11 Internal stress of AL2, BL1, and BL2 at displacement of 25×10^{-3} rad

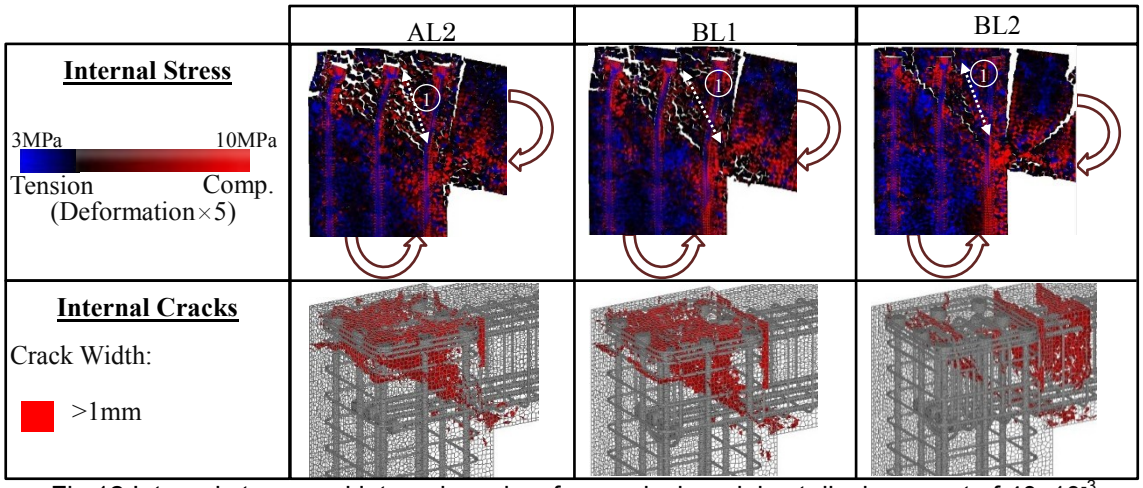

Fig.12 Internal stress and internal cracks of numerical models at displacement of 40×10^{-3}

exist in the beam column joint that causes the load does not decrease significantly. Based on the simulation results, in case of BL2, the load does not decrease significantly because the diagonal compressive stresses still exist in the beam column joint as the result of the restriction of the stirrups.

At this displacement, cracks are also predicted along the end of the anchorage plates because the interface between the anchorage plates and concrete is weak in tension (⑤). These cracks, diagonal cracks and cracks along the end of the anchorage plates, are connected each other that causes major cracks in the beam column joint with mechanical anchorages. The causes of the major cracks in the beam column joint have been revealed through simulation results.

4.4 Internal Cracks

Fig. 12 shows the internal stress and internal cracks of numerical models at the displacement of 0.04 rad. Cracks are predicted at the end of the anchorage plates of the longitudinal bars of the column. As described above, diagonal cracks open easily in case of AL2 and BL1. As diagonal cracks open easily, cracks at the top surface of the beam column joint open that causes damage at the top surface and these cracks are connected each other. In case of BL2, the confinement provided by stirrups along the anchorages prevents the diagonal cracks to open wider so that cracks at the top surface of the beam column joint are difficult to open. It indicates that there are two effects of stirrups provided along the anchorages, i.e. to prevent diagonal cracks to open wider and to prevent cracks at the top surface of the beam column joint to open by providing the confinement effect. It is also confirmed based on the simulation results that the cause of the second diagonal cracks, propagating from the anchorage plates of middle longitudinal bars of the column to the corner of the beam column joint (①), is the diagonal compressive stresses developing from the anchorage plates of middle longitudinal bars of the column, as the result of the bearing stress, to the compression zone of the beam.

5. CONCLUSIONS

(1) RBSM can simulate the different failure pattern due to the different local stirrups arrangement. Based on the simulation results, the increase of the capacity of BL2 is due to the increase of the bond performance along the development length of anchorages and confining diagonal stresses caused by stirrups.

(2) It is confirmed based on the simulation results that when stirrups are provided along the anchorage, stirrups can restrict the opening of diagonal cracks. Therefore, diagonal compressive stresses still remain and avoid the cracking near the anchorages. As the result, flexural failure occurs.

(3) The failure process of beam column joints with mechanical anchorages has been revealed through the study of internal stress and crack pattern of RBSM.

REFERENCES

[1] Japan Society of Civil Engineers, "Recommendations for Design, Fabrication and Evaluation of Anchorages and Joints in Reinforcing Bars," Concrete Library 128, 2007. (in Japanese)

[2] Yoshimura, M.; Kiyohara, T.; Tasai, A.; Kusunoki, K., "Experimental Study of Performance Improvement of Knee Joints with Mechanical Anchorage," Proceedings of Japan Concrete Institute, Vol.34, No.2, 2012. (in Japanese)

[3] Wang, T.; Eddy, L.; Nagai, K., "Numerical Simulation of Failure of Beam Column Joint with Mechanical Anchorage by 3D Discrete Analysis,"6th Asia-Pacific Young Researchers and Graduates Symposium, 2014.

[4] Kawai, T., "New Discrete Models and Their Application to Seismic Response Analysis of Structure," Nuclear Engineering and Design, 48, 207-229. 1978.

[5] Nagai, K.; Sato, Y.; Ueda, T., "Mesoscopic Simulation of Failure of Mortar and Concrete by 3D RBSM," J. Adv. Conc. Technol., 3(3), 385-402. 2005.

[6] Nagai, K.; Hayashi, D.; Eddy, L., "Numerical Simulation of Failure of Anchorage with Shifted Mechanical Anchorage Bars by 3D Discrete Model," J. Adv. in Structural Engineering, Vol.17, 861-870. 2014.